의학박사 학위논문

Clinicopathological analysis of *ROS1* gene alterations and immunohistochemistry screening for *ROS1* gene rearrangement in non-small cell lung cancer

비소세포폐암에서 ***ROS1*** 유전자 변이의 임상병리학적 특성 및 유전자 전위의 선별진단법 개발

2015년 08월

서울대학교 대학원

의학과 병리학전공

JIN YAN

비소세포폐암에서 *ROS1* 유전자 변이의 임상병리학적 특성 및 유전자 전위의 선별진단법 개발

지도교수 정진행

이 논문을 의학박사학위논문으로 제출함

2015년 4월

서울대학교 대학원

의학과 병리학전공

JIN YAN

JIN YAN 의 박사학위논문을 인준함

2015년 6월

위 원 장 _____ **(인)**

부 위 원 장 _____ **(인)**

위 원 _____ **(인)**

위 원 _____ **(인)**

위 원 _____ **(인)**

Clinicopathological analysis of *ROS1* gene alterations and immunohistochemistry screening for *ROS1* gene rearrangement in non-small cell lung cancer

by

JIN YAN

A Thesis Submitted to the Department of Pathology in Partial Fulfillment of the Requirements for the Degree of Doctor of Philosophy in Pathology at Seoul National University College of Medicine

June 2015

Approved by Thesis Committee:

Professor _____ **Chairman**

Professor _____ **Vice chairman**

Professor _____

Professor _____

Professor _____

Abstract

Clinicopathological analysis of *ROS1* gene alterations and immunohistochemistry screening for *ROS1* gene rearrangement in non-small cell lung cancer

JIN YAN

Department of Pathology

The Graduate School

Seoul National University College of Medicine

Introduction: *ROS1* rearrangement, found in a subset of lung cancers, have therapeutic significance, as *ROS1*-rearranged tumors are sensitive to ALK kinase inhibitors. This study sought to evaluate the clinicopathological implications of *ROS1* gene alterations and the histomorphological characteristics of *ROS1*-rearranged tumors, especially micropapillary and aerogenous spread growth, and to investigate the usefulness of ROS1 immunohistochemistry as a diagnostic test for *ROS1* rearrangement.

Methods: Characterization of *ROS1* gene alterations using fluorescent *in situ* hybridization, and characterization of ROS1 and E-cadherin protein expression using immunohistochemistry were performed in 754 non-small cell lung cancer (NSCLC) surgical samples.

Results: *ROS1* rearrangement was identified in ten patients (1.3%, NSCLC; 1.9%, adenocarcinoma). Histologically, all ten *ROS1*-rearranged tumors harbored an adenocarcinoma component. Importantly, *ROS1* rearrangements were highly associated with micropapillary components ($p < 0.001$), aerogenous spread status ($p = 0.002$), and loss of E-cadherin expression ($p = 0.049$). Kaplan-Meier survival curves

with log-rank test showed that *ROS1* rearrangement was significantly associated with a higher risk of tumor recurrence ($p = 0.024$). Nine of the ten *ROS1*-rearranged tumors showed moderate-to-strong ROS1 immunoreactivity, with a 100–300 H-score range (median, 240), whereas most *ROS1* wild-type cancers (73.3%) lacked detectable immunoreactivity (H-score range, 0–240; median, 0). The criterion that best differentiated between *ROS1*-rearranged and *ROS1* wild-type tumors was an H-score of ≥100, with a sensitivity and specificity of 90% and 93.5%, respectively. On the other hand, *ROS1* gene copy number gain (CNG) was found in 4.8% (18/375) of the tumors. *ROS1* gene CNG was significantly associated with shorter disease-free survival (DFS, 12 *vs.* 58 months; $p = 0.003$) and shorter overall survival (OS, 40 *vs.* 67 months; $p < 0.001$) compared to that observed in the group without CNG. Multivariate analysis confirmed that *ROS1* gene CNG was significantly associated with poorer DFS (hazard ratio [HR] = 2.16, 95% confidence interval [CI] = 1.22–3.81, $p = 0.008$), and poorer OS ([HR] = 2.53, 95% [CI] = 1.31–4.89, $p = 0.006$).

Conclusion: This study demonstrated that *ROS1* gene rearrangement was detected in 1.9% of surgically resected adenocarcinoma. The patients harboring *ROS1*-rearrangement showed shorter DFS. *ROS1*-rearranged lung adenocarcinoma exhibited distinct morphological and clinicopathological features, including high prevalence of cribriform and/or micropapillary pattern with aerogenous spread status and decreased membranous E-cadherin expression. Cutoff value of H-score 100 best predicts *ROS1* rearrangement. On the other hand, *ROS1* gene CNG is an independent indicator of poor prognosis in surgically resected NSCLC.

Keywords: Lung cancer, *ROS1* gene alteration, histomorphology, immunohistochemistry

Contents

List of Tables

List of Figures

List of Abbreviations and Symbols

NSCLC	Non–small cell lung cancer
ADC	Adenocarcinoma
EGFR	Epidermal growth factor receptor
TKIs	Tyrosine kinase inhibitors
ALK	Anaplastic lymphoma kinase
RET	Rearranged during transfection
ROS1	C-ros oncogene 1
PIK3	Phosphoinositide-3 kinase
AKT	V-akt murine thymoma viral oncogene homolog 1
mTOR	Mechanistic target of rapamycin
MAPK	Mitogen activated protein kinase
ERK	Extracellular signal-regulated kinase
SHP	Src-homology 2 domain-containing phosphatase
CNG	Copy number gain
IHC	Immunohistochemistry

FISH	Fluorescence *in situ* hybridization
RT-PCR	Reverse-transcription polymerase chain reaction
p-Stage	Pathologic stage
DFS	Disease-free survival
OS	Overall survival
WHO	World Health Organization
IASLC	International Association for the Study of Lung Cancer
ATS	American Thoracic Society
ERS	European Respiratory Society
FFPE	Formalin-fixed and paraffin-embedded
CEP6	Centromere enumeration probe 6
HR	Hazard ratio
CI	Confidence interval

Introduction

1. Non-small cell lung cancer and therapy

Lung cancer is the most commonly diagnosed cancer and the leading cause of cancer-related death worldwide (1). Approximately 85% of patients have non-small cell lung cancer (NSCLC), and most advanced patients are not amenable to curative therapy. For these patients, cytotoxic chemotherapy offers a modest extension of survival. Over the past two decades, modifications of chemotherapy combinations, the addition of monoclonal antibodies, including bevacizumab and cetuximab, and the incorporation of histological subtypes into treatment decisions have added incrementally to the survival of patients with advanced NSCLC. However, therapeutic outcomes appear to have reached a bottle-neck, with response rates of 20% to 35% and a median survival of 8 to 12 months (2, 3).

Recently, the transition from cytotoxic chemotherapy to molecularly targeted cancer drug discovery and development has resulted in an increasing number of successful therapies that have impacted the lives of a large number of lung adenocarcinoma (ADC) patients (4). The first successful example of molecular targeted therapy involved the epidermal growth factor receptor (EGFR). Lung tumors harboring specific activating mutations in the EGFR kinase domain were highly sensitive to the EGFR tyrosine kinase inhibitors (TKIs) erlotinib, gefitinib and afatinib (5). With the exception of the *EGFR* mutation, several chromosomal rearrangement have been identified in lung ADC, including *ALK (anaplastic lymphoma kinase)*, *RET (rearranged during transfection*), and *ROS1* (*c-ros oncogene*

1), which can lead to the expression of oncogenic and potentially "druggable" fusion kinases.

2. *ROS1* gene rearrangement

ROS1 is a receptor tyrosine kinase with homology to the insulin receptor (6). The *ROS1* oncogene was initially identified as the cellular homolog of the transforming v-ros sequence from the avian sarcoma RNA tumor virus (7). The *ROS1* gene is located at chromosome 6q22. Dysregulated ROS1 may occur as a result of *ROS1* gene fusion, overexpression, or mutations (8). Aberrant ROS1 kinase activity leads to activated downstream signaling of several oncogenic pathways that control cell proliferation, survival, and cell cycling, including the phosphoinositide-3 kinase (PI3K)/v-akt murine thymoma viral oncogene homolog 1 (AKT)/mechanistic target of rapamycin (serine/threonine kinase) (mTOR) pathway, the signal transducers and activators of transcription-3 pathway, the RAS-mitogen activated protein kinase/extracellular signal-regulated kinase (RAS-MAPK/ERK) pathway, and the Src-homology 2 domain-containing phosphatase (SHP)-1 and -2 pathway, (8, 9). *ROS1* proto-oncogene receptor tyrosine kinase is activated by chromosomal rearrangement in a variety of human cancers, including NSCLC (10), glioblastoma (11), cholangiocarcinoma (12, 13), ovarian cancer (14), gastric cancer (15), and colorectal cancer (16). *ROS1* gene rearrangement were first identified in NSCLC in 2007 (10) and have since been described in 1% to 2% of patients with NSCLC (17, 18). At least nine fusion variants have been reported in NSCLC, including *SLC34A2, CD74, EZR, LRIG3, SDC4, TPM3, FIG, CCDC6,* and *KDELR2* (10, 19-21). Previous studies have reported that *ROS1* is evolutionarily related to *ALK* (22, 23). The mouse ALK and ROS1 proteins share most amino acid homology within the kinase domain (24). These

major discoveries led to the hypothesis that ALK inhibitors act as ROS1 inhibitors. As expected, the in vitro studies and preliminary data from a clinical trial suggested that ALK inhibitors effectively suppress the growth of *ROS1*-rearranged tumors (22, 25). Since *ROS1*-rearranged tumors are sensitive to most ALK inhibitors, their identification may be of great importance for both patient- and tumor-specific therapeutic intervention (22).

In addition, *ALK* copy number gain (CNG) and amplification have been reported as frequent events in NSCLC (26, 27). In an earlier study, our group showed that *ALK* CNG was more frequently identified in metastatic lesions than in primary tumors and was related to shorter progression-free survival and decreased overall survival rates (28). Although the implications of *ROS1* rearrangement have been generally understood, there have been no reports to date describing the clinical implications of *ROS1* gene CNG or a discussion of whether patients with *ROS1* gene CNG respond to treatment.

3. Characterization of *ROS1* gene rearrangement

Recently, several studies reported that the clinicopathological characteristics of patients with *ROS1*-rearranged NSCLC are remarkably similar to those of patients with *ALK*-rearranged NSCLC, including young age of onset with non-smoking or light smoking history (22, 24, 29). In addition, most *ALK* and *ROS1*-rearranged lung cancers focally exhibit “solid signet-ring cell” or “mucinous cribriform” patterns (30, 31) and decreased membranous E-cadherin expression in *ALK*-rearranged lung cancers has been reported (32). However, the limited numbers of patients with *ROS1*-rearranged lung cancers has hindered the comprehensive characterization of histological and clinicopathological features of these cancers, and there have been no

reports on the status of E-cadherin expression in *ROS1*-rearranged tumors.

4. Detection method of *ROS1* gene rearrangement

Methods that allow the detection of *ROS1* rearrangements include fluorescence *in situ* hybridization (FISH), reverse-transcription polymerase chain reaction (RT-PCR), and immunohistochemistry (IHC). Among those detection methods, FISH is the most commonly used to detect *ROS1* rearrangement; however, this method is complex and has limitations in terms of cost and throughput, making it impractical for screening large numbers of patients for the detection of rare events(33). Although a benefit of RT-PCR is that it allows for precise identification of the sequence variant, the technology requires previous knowledge of fusion variants and the use of multiple primer pairings, and therefore cannot be used to detect novel fusion variants (33). IHC is a less expensive alternative and is still commonly used in pathology; however, despite several attempts to improve the accuracy of ROS1 IHC assays for lung cancer, the utility of IHC to screen *ROS1* gene rearrangement is controversial (34, 35). Therefore, further work is required to develop suitable guidelines for the interpretation of results from IHC assay, in order to establish a suitable ROS1 IHC assay for sensitive and specific *ROS1* rearrangement identification.

The aim of this study was 1) to evaluate the clinicopathological implications and histomorphology of *ROS1*-rearranged tumors, 2) to determine the criteria can be used for the detection of *ROS1* rearrangement by ROS1 IHC, and 3) to clarify the prognostic impact of *ROS1* gene CNG in surgically resected NSCLC.

Materials and Methods

1. Patients and samples

Tumor samples were collected from 754 patients who underwent surgical resection for NSCLC at Seoul National University Bundang Hospital between May 2003 and December 2012. Clinical data, including age, sex, smoking history, pathological stage (p-Stage), disease-free survival (DFS), and overall survival (OS), were retrieved from the patients' medical records. Smoking status was defined as never-smokers (<100 cigarettes over the lifetime) and smokers. The tumor p-Stage was characterized using the new 7th Edition of the Union for International Cancer Control-American Joint Committee on Cancer staging system (UICC/AJCC) (36). All patients had a pathological diagnosis of primary lung cancer defined according to the 2015 World Health Organization (WHO) classification (37). The histology of all *ROS1* rearrangement cases were analyzed in detail. OS was measured from the date of lung cancer surgery until the time of death, and DFS was measured from the date of surgery until disease progression or death. This study was approved by the Institutional Review Board (IRB) of Seoul National University Bundang Hospital.

2. Construction of tissue microarrays

All formalin-fixed paraffin-embedded (FFPE) tumors were assembled into tissue microarrays (TMA) using 2-mm diameter cores sampled from the most representative areas of the tumor. Five cores were sampled and included in the TMA block from

each patient. Serial sections were cut and examined using both IHC and FISH.

3. *ROS1* gene rearrangement and CNG

FISH assay was performed on the TMA sections using a ROS1 probe (6q22 ROS1 Break Apart FISH Probe RUO Kit, Vysis, Abbott Molecular, USA) and centromere enumeration probe 6 (CEP 6 SpectrumOrange DNA probe kit, Vysis, Abbott Molecular, USA), according to manufacturer's instructions. To identify *ROS1* gene rearrangement, the probe mixture was prepared in a microcentrifuge tube as follows: 7 μL LSI/WCP Hybridization Buffer, 1 μL 6q22 ROS1 (Tel Break-Apart) SpectrumOrange Probe RUO, 1 μL 6q22 ROS1 (Cen) SpectrumGreen Probe RUO, and 1 μL purified water. Signals for each probe were evaluated under a microscope equipped with a triple-pass filter (diamidino-2-phenylindole/ Green/ Orange; Abbott Molecular), using an oil immersion lens.

At least 100 non-overlapping tumor cells per core were evaluated. Fused orange (5' end) and green (3' end) signals appeared yellow and indicated the colocalization of the orange and green signals. FISH cells were considered positive (rearranged) if a split occurred one or more signal widths apart between the orange and green signals, or if there was a single green signal without a corresponding orange signal in conjunction with fused and/or split signals (38). A case was considered negative if there was a single orange signal without a corresponding green signal in conjunction with fused and/or split signals. A case was considered positive for *ROS1* gene rearrangement if more than 15% of tumor cells showing split or isolated green signals (35). In addition to the *ROS1* rearrangement, increased *ROS1* gene copy number also occurred. *ROS1* gene CNG was defined as *ROS1* $\geq$ 4 copies per nucleus in > 40% of

cells and *ROS1* gene amplification was defined as the ratio of *ROS1* gene to CEP6 ≥ 2 or ≥15 copies of *ROS1* gene per cell in ≥10% of analyzed cells. The CEP6 gain was defined as mean CEP6 ≥ 3 copies per nucleus (39, 40).

4. ROS1 and E-cadherin protein expression

IHC staining was performed on FFPE TMA sections. Four-micrometer thick tissue sections were stained using a Ventana automated immunostainer (Ventana Medical Systems, Tucson, AZ, USA), according to the manufacturer's protocol. Briefly, the slides were dried at 60℃ for 1h and deparaffinized using EZ Prep (Ventana Medical Systems) at 75℃ for 4 min. Cell conditioning (heat pretreatment) was performed using CC1 solution containing Tris/Borate/EDTA at 100℃ for 20 min. Slides were incubated with anti-ROS1 antibody (D4D6, 1:50; Cell Signaling Technology, Danvers, MA, USA) and E-cadherin (1:100; SPM471; Thermo Fisher Scientific, MA, USA) for 32 min at 37℃. Signals were detected using OptiView DAB IHC Detection Kit (Ventana Medical Systems). Counterstaining was performed with hematoxylin I (Ventana Medical Systems) for 4 min at room temperature.

Immunoreactivity was examined under a microscope (Olympus BX53, Tokyo, Japan). ROS1 protein expression was scored on the basis of staining intensity and proportion of positive cells, where an intensity score of 1+ was defined as "reactivity only detectable at high magnification" (objective lens, ×20–×40). More intense reactivity was classified as moderate (score, 2+) or strong (score, 3+) based on ease of detection at low magnification (objective lens, ×4). The H-score, in the range of 0–300 was calculated by multiplying the intensity score and fraction score (34). For E-cadherin, the membranous pattern was scored based on the intensity (0, negative; 1,

weak; 2, moderate; 3, strong) and completeness (0–100%) of the staining. A total score range of 0 to 300 was generated for each sample, where 0 to 100 was defined as decreased E-cadherin expression and 101 to 300 was classified as normal E-cadherin expression (32). All slides were evaluated blinding from the results of FISH assay.

5. Histological analysis of *ROS1*-rearranged tumors

Samples positive for *ROS1* rearrangement were further analyzed by histology. An average of 8 slides (range: 2-14 slides) from each case was reviewed. Hematoxylin and eosin (H&E) stained slides were available for all 10 cases with *ROS1* rearrangement. All invasive ADC were categorized as lepidic, papillary, acinar, micropapillary, or solid predominant according to the new International Association for the Study of Lung Cancer/American Thoracic Society/European Respiratory Society (IASLC/ATS/ERS) classification (41). The following histological parameters were evaluated: tumor size, p-Stage, predominant growth pattern, any existing growth pattern, aerogenous spread status, and invasion status (pleural, vascular, or lymphatic). Aerogenous spread is morphologically defined as the presence of non-attached micropapillary cell clusters in the alveolar space seen at a distance of at least one low power field from the main mass. Recent studies have shown that most of *ROS1*-rearranged lung cancers focally exhibit a “solid signet-ring cell” or “mucinous cribriform” patterns (30). Particular attention was paid to the presence or absence of any solid growth patterns containing signet-ring cells and cribriform structures associated with abundant extracellular mucus.

6. Analysis of additional ADC-associated mutations and rearrangement

Genomic DNA was extracted from FFPE tissues. After deparaffinization with xylene, tissue sections were stained with H&E, and target lesions were selectively dissected to minimize contamination with normal tissue. Genomic DNA was isolated using the QIAamp DNA Mini Kit (Qiagen, Hilden, Germany) according to the manufacturer's instructions. Samples were analyzed for *EGFR* mutations within exons 18 to 21 and *KRAS* mutations at codons 12, 13, and 61 using PCR and direct DNA sequencing or pyrosequencing methods (42, 43). *ALK* rearrangement was analyzed by FISH using a Vysis break-apart rearrangement probe for *ALK* (Abbott Molecular, Abbott Park, IL) (44).

7. Statistical analysis

Statistical analyses were performed using the software package Statistical Package for Social Sciences, version 19.0, for Windows (SPSS, Chicago, IL, USA). To analyze the correlation between clinicopathological parameters, Pearson's chi-square or Fisher's exact tests were used. Survival curves were determined using the Kaplan-Meier method, and the significance of differences between these curves was determined using the log-rank test. Multivariate survival analyses were performed using the Cox proportional hazards model to evaluate whether a parameter was an independent prognostic factor for survival. All statistical values were determined using two-tailed statistical analyses, and p values of < 0.05 were considered to indicate a statistically significant difference.

Results

1. Patient and tumor characteristics

The clinical characteristics of the patients are summarized in Table 1. The patient cohort from whom tumor samples were obtained included 253 women (33.6%) and 501 men (66.4%), with a median age of 66 years (range, 23–85 years). Of the 754 patients, 303 patients (40.2%) were non-smokers and 451 were smokers (59.8%; 337 current-smokers and 114 ex-smokers). Histological characterization of tumors revealed that 469 samples were ADC (62.2%), 254 were squamous cell carcinomas (33.7%), and 31 were other subtypes of NSCLC (4.1%; 11 adenosquamous carcinoma, 7 large cell neuroendocrine cell carcinoma, 6 pleomorphic carcinoma, 2 large cell carcinoma, 2 atypical carcinoid tumor, 2 carcinoid tumor, 1 carcinosarcoma). Characterization of the pathological stage of each tumor indicated that 193 patients were in stage IA, 168 patients were in IB, 131 patients were in IIA, 57 patients were in IIB, 156 patients were in IIIA, 16 patients were in IIIB, and 33 patients were in IV.

2. *ROS1* rearrangement by FISH

ROS1 rearrangement were identified in ten patients (10/754 (1.3%) in NSCLC, 9/469 (1.9%) in ADC) (Figure 1). The demographic and clinical characteristics of the patients with *ROS1* rearrangement are summarized in Table 2. Patients presenting with *ROS1*-rearranged tumors consisted of three men and seven women with a mean age of 55.5 years (range: 45–80). Of the 10 patients, seven were non-smokers and

three were smokers (two were ex-smokers and one was a current-smoker who consumed approximately 15 pack-years). Histological analysis revealed that nine patients presented with ADC and one with a pleomorphic carcinoma composed of both adenocarcinomatous and sarcomatous components. *ROS1* rearrangement was found in both the adenocarcinomatous and sarcomatous components of the tumor. *ROS1* rearrangement was more prevalent in younger women (age: $p = 0.042$; sex: $p = 0.014$) (Table 3). Rearrangement also tended to be associated, albeit non-significantly, with pleural invasion ($p = 0.053$), with advanced pathological stage ($p = 0.074$), and with people who did not smoke ($p = 0.053$) (Table 3). No mutations in *EGFR or ALK* gene rearrangement were observed in the *ROS1*-rearranged samples; however, a single *ROS1*-positive sample harbored a *KRAS* mutation (Table 2). Seven of the ten patients suffered from relapse after the initial surgery.

3. Pathological features of *ROS1*-rearranged NSCLC

Meticulous histological examination of the both *ROS1*-rearranged and wild-type tumors was performed to analyze tumor morphology, severity, and composition. The median tumor size was 31.5 mm (range, 25–48 mm). According to the pathological stage, four, one, three, and two of the cases were in p-Stage I, II, III, and IV, respectively. In the nine *ROS1*-rearranged ADC tumors, the predominant growth pattern was solid in three cases, acinar in three, micropapillary in two, and lepidic in one. A solid growth pattern containing signet-ring cells was at least focally present in three cases (Figure 2A). The amount of solid signet-ring cell patterns ranged from 5% to 90% of the tumor volume. A cribriform structure was identified at least focally in nine cases and accounted for 5–98% of the tumor volume (Figure 2B). Importantly, a

micropapillary pattern was observed in most *ROS1*-rearranged tumors (8/10; range, 2–85%) and was statistically more common than in *ROS1* wild-type tumors ($p < 0.001$) (Figure 2C). Moreover, all ten *ROS1*-rearranged tumors showed aerogenous spread status of tumor cells (Figure 2D). Aerogenous spread status was significantly more prevalent in tumors with *ROS1* rearrangement than in *ROS1* wild-type tumors ($p = 0.002$). Pleural invasion, vascular invasion, and lymphatic invasion were observed in seven, three, and six of *ROS1*-rearranged tumors, respectively.

4. ROS1 protein expression

IHC analyses were performed on all 754 cases, and ROS1 immunoreactivity was detected in 208 (27.6%) of these. ROS1 protein was faintly detected in the cytoplasm of macrophages and reactive type II pneumocytes, and in normal non-neoplastic bronchial epithelial cells, whereas in tumor cells, ROS1 protein was detected predominantly in the cytoplasm with variable staining intensity (Figure 3A). In nine of ten *ROS1*-rearranged cancers, diffuse but moderate-to-strong ROS1 immunoreactivity was observed (relative staining intensity scores: six samples with 3+, two samples with 2+, and one sample with 1+), with an H-score range of 100–300 (median, 240) (Figure 3B), except for one case with an H-score of 0. In contrast, most *ROS1* wild-type cancers (73.3%) lacked detectable immunoreactivity; the remaining cases (199, 26.7%) presented some degree of staining; however, the staining was mostly weak or focally distributed. The median H-score for the entire *ROS1* wild-type group was 0 (range, 0–240). Of these, 171 (86.0%) showed low immunoreactivity (H-score range, 0–100), 26 (13.0%) showed moderate immunoreactivity (H-score range, 0–100), and 2 (1.0%) showed H-score 240.

5. E-cadherin protein expression

E-cadherin expression was accentuated toward the apical and basolateral regions of the tumor cell membrane (Figure 4). Importantly, decreased E-cadherin expression was observed in all *ROS1*-rearranged tumors and was significantly more common in *ROS1*-rearranged tumors than in *ROS1* wild-type tumors (p = 0.049). Decreased E-cadherin expression was more frequently observed in *ROS1*-rearranged tumors than other genotypes (*EGFR* mutated group: p = 0.046; *KRAS* mutated group: p = 0.036; *EGFR/KRAS/ALK/ROS1* negative ADC: p = 0.018), but with similar frequency to that observed in *ALK*-rearranged tumors (p = 0.096).

6. Survival analysis

At the time of analysis, the number of tumor recurrences was 280 (37.1%, 280/754), and the number of cancer-specific deaths was 143 (19.0%, 143/754). Follow-up data were available for all patients at a median of 36 months (range, 1–84 months) after surgery. *ROS1* rearrangement was significantly associated with shorter DFS (median DFS, 27 *vs.* 55 months; p = 0.024), but not associated with OS (median OS, 52 *vs.* 68 months; p = 0.985). To evaluate whether *ROS1* rearrangement in NSCLC is an independent predictor of survival, a multivariate analysis using the Cox proportional hazard model was performed. However, *ROS1* rearrangement was not an independent prognostic factor (hazard ratio [HR] = 1.626, 95% confidence interval [CI] = 0.754–3.506, p = 0.215).

In the ADC cohort, mutational status for *EGFR/KRAS/ALK/ROS1* was available in 385 cases including 221 *EGFR* mutations, 24 *KRAS* mutations, *26 ALK*

rearrangements, 9 *ROS1* rearrangements, and 105 *EGFR/KRAS/ALK/ROS1* negative. *ROS1* rearranged tumors showed significantly shorter DFS than *ROS1* wild-type tumors (median DFS, 23 *vs.* 61 months; $p = 0.011$) (Figure 5A), but not OS (median DFS, 51 *vs.* 65 months; $p = 0.919$). In addition, *ROS1* rearranged tumors had significantly worse DFS than the *EGFR/KRAS/ALK/ROS1*negative group ($p = 0.017$) (Figure 5B).

7. Correlation of ROS1 IHC and ROS1 rearrangement by results

To determine the correlation between FISH detection of *ROS1* rearrangement and IHC determination of ROS1 expression, the presence or absence of *ROS1* rearrangement with the H-score, as well as the extent and intensity of IHC staining were compared. A range of criteria (H-scores: 50, 80, 100, 150, and 200; extent (%): 10%, 20%, 50%, and 75%; intensity: 1+, 2+, and 3+) was tested to determine an optimal set of diagnostic conditions that best differentiated *ROS1*-rearranged and *ROS1* wild-type tumors and to calculate the sensitivity and specificity for each condition. The best differentiation was achieved using an H-score criterion of ≥ 100, in which the sensitivity and specificity of detection and differentiation were 90% and 93.5%, respectively (Table 4).

8. *ROS1* gene and CEP6 CNG

The median *ROS1* gene copy number per nucleus was 2.30 (range, 1.38–4.56) (Figure 6A). *ROS1* gene CNG was detected in 18 cases (18 of 372, 4.8%), but gene amplification was not identified. *ROS1* gene rearrangement was not observed in any

of those cases. *ROS1* gene CNG status was tended to be more common in men than in women (p = 0.071) and in squamous cell carcinoma than in other histological subtypes (p = 0.096). There was no correlation between *ROS1* gene CNG and high protein expression. To determine the prognostic impact of *ROS1* gene CNG, survival analyses were performed using Kaplan-Meier and Cox proportional hazard models for DFS. The results of the Kaplan-Meier univariate analysis indicated that *ROS1* gene copy number status, tumor stage, and pleural invasion all reached significance. As illustrated in Figure 7, the presence of *ROS1* gene CNG was significantly associated with a higher risk of recurrence and shorter OS (median DFS, 12 *vs.* 58 months; p = 0.003; median OS, 40 vs. 67 months; $p < 0.001$). Multivariate analysis indicated that *ROS1* gene CNG was an independent factor of poor prognosis factor for DFS (hazard ratio [HR] = 2.16, 95% confidence interval [CI] = 1.22–3.81, p = 0.008) and OS ([HR] = 2.53, 95% [CI] = 1.31–4.89, p = 0.006) (Table 5). To determine the correlation between *ROS1* gene CNG and ROS1 protein expression, statistical analysis was performed using Pearson's analysis. No correlation was observed between *ROS1* gene CNG and high expression of ROS1 protein (H-score $\geq$100).

The CEP6 status was analyzed in 350 cases. The median CEP6 copy number per nucleus was 2.74 (range, 1.62–7.6) (Figure 6B). The median *ROS1*:CEP6 ratio was 0.88 (range, 0.27–1.7). CEP6 gain was observed in 28.8% (101/350) and associated with pleural invasion (p = 0.003) as well as lymphatic invasion (p = 0.013). In addition, CEP6 gain status tended to be more common in ADC histological subtype (p = 0.077). Of 18 patients with a *ROS1* gene CNG, nine (50%) were found to have CEP6 gain, but there was no statistically positive correlation between *ROS1* gene CNG and CEP6 gain.

Discussion

This purpose of this study was to determine the clinicopathological implications of *ROS1*-rearranged and *ROS1* gene CNG tumors, and also sought to determine the sensitivity and specificity of an IHC screening method used to predict *ROS1* rearrangement. The main findings are as follows: (1) the prevalence of *ROS1* rearrangement (1.9%) in a surgically resected lung ADC population was higher than that in overall surgically resected NSCLC (1.3%); (2) *ROS1*-rearranged tumors were more likely to show a micropapillary growth pattern and aerogenous spread status; (3) *ROS1*-rearranged tumors showed decreased membranous E-cadherin protein expression more frequently and poor DFS by univariate analysis; (4) an H-score of 100 yielded maximum sensitivity and specificity in differentiating between tumors that contained *ROS1* rearrangement and tumors that did not; (5) *ROS1* gene CNG status was prone to be more common in male patients and in cases with squamous histology; and (6) *ROS1* gene CNG is an independent factor of poor prognosis in unselected, surgically resected NSCLC patients.

Histological analyses of lung carcinoma form an important basis of treatment decisions. Furthermore, morphological features of lung ADC, determined by histology, correlated with common molecular alterations associated with tumor subtypes (29, 41). Examples of these associations include *EGFR* mutations with lepidic and papillary patterns (45, 46), and *KRAS* mutations with solid and invasive mucinous ADC subtypes (47, 48). Previous studies demonstrated that histological features of *ROS1*-rearranged tumors are similar to those of *ALK*-rearranged tumors (30, 49). In this study, *ROS1*-rearranged tumors also had similar histological features, including

solid and/or acinar predominant growth patterns with frequent cribriform morphologies. Interestingly, micropapillary component and aerogenous spread status were highly associated with *ROS1* rearrangement when compared to *ROS1* wild-type tumors. The micropapillary pattern of tumor cells is a marker of aggressive tumor biology characterized by high rates of recurrence and poor survival, even in completely resected early-stage tumors (50, 51). Aerogenous spread status is a phenomenon of a tumor that metastasizes through the alveolar spaces and only occurs when cancer cells detached from the basement membrane (52). The high association of these findings with *ROS1*-rearranged tumors underscores the need for further studies on E-cadherin protein expression because loss of E-cadherin, a crucial cell-cell adhesion molecule, breaks down cell-cell contact, owing to which malignant cells detach from the epithelial-cell layer, resulting in tumor motility (53). In this study, we also performed IHC of other epithelial-mesenchymal transition (EMT) markers including vimentin, snail, β-catenin, and matrix metalloproteinase (MMP) protein expression. Among those EMT markers, only E-cadherin expression showed significant difference between *ROS1*-rearranged and wild-type lung tumors, suggesting that E-cadherin loss play important roles in EMT at least in lung cancer. Taken together, these histological findings with decreased membranous E-cadherin expression may be associated with shorter DFS of the patients harboring *ROS1*-rearrangement. To the best of my knowledge, this is the first report of decreased membranous E-cadherin expression in ROS1-rearranged NSCLC.

Several studies have evaluated whether *ROS1* gene rearrangement influence patient survival, but the results are controversial (30, 54, 55). A few studies have reported that no significant difference in overall survival was observed between patient groups with *ROS1* rearranged and wild-type tumors (30, 54). Recently, Lee et

al. reported that patients with *RET/ROS1*-rearranged tumors have longer recurrence-free survival than do *EGFR/KRAS/ALK/ROS1/RET*-negative groups (56). In contrast to their results, my study indicated that *ROS1* rearrangement ADC was significantly associated with a higher risk of tumor recurrence than *ROS1* wild-type or *EGFR/KRAS/ALK/ROS1*-negative ADC. Frequent micropapillary growth pattern and aerogenous spread status with decreased membranous E-cadherin expression in *ROS1*-fusion positive patients in this study supports the finding that DFS is worse in these patients than in the *ROS1*-fusion negative group. Owing to the limited number of cases of *ROS1*-rearranged NSCLC, large-scale meta-analysis is required to evaluate the clinical implications of *ROS1* rearrangement.

Consistent with earlier observations (34, 35, 49, 57), these results support the use of IHC by demonstrating high sensitivity (90%) and specificity (93.5%) for detecting and differentiating *ROS1*-rearranged cancers. Uncharacteristically, one *ROS1*-rearranged sample showed no ROS1 immunoreactivity. The failure of immunoreaction could be attributed to the age of the tissue block, which was >10 years, whereas the age of IHC-positive tissue blocks from *ROS1*-rearranged tumor samples was <7 years. Because immunohistochemistry is affected by many preanalytical variables, including fixation duration, type of fixative, age of the tissue block, and sample storage conditions, ROS1 IHC status ideally should be determined at the time of excision of primary lesions.

In the present study, *ROS1* gene CNG were found in 18 cases (4.8%) and prone to be more common in male patients ($p = 0.071$) and squamous histology ($p = 0.096$). However, *ROS1* rearrangement was not observed in any of these cases. These findings are different from the clinicopathologic characteristics of *ROS1* gene rearrangement in which female gender and ADC histology showed predominance (25, 30).

Consequently, it is possible that the occurrence of *ROS1* gene CNG does not rely on gene rearrangement. In the present study, the survival analysis demonstrated that *ROS1* gene CNG was an independent factor of poor prognosis of DFS and OS.

Several studies have already reported that the *ALK* gene CNG and amplifications are frequent events in NSCLC, and that lines with high *ALK* copy number cells have increased sensitivity for crizotinib (27). In contrast, Camidge et al., on exploring the details of variation in native *ALK* copy number, proposed that the mean *ALK* copy number ranged from 2.1 to 6.9 copies in cell lines and did not correlate with crizotinib sensitivity (58). It is necessary to consider the implications of *ROS1* gene CNG because of the similarities between the *ALK* gene and the *ROS1* gene. Further study is needed to accurately determine the therapeutic potential of *ROS1* gene CNG. The limitation of this study includes the small sample size of *ROS1* gene rearrangement, which was not sufficient to compare differences in OS and in DFS. On the other hand, the major strength of this study was that some of the clinical implications of the *ROS1* gene CNG were evaluated; to the best of my knowledge, this is the first report of *ROS1* gene CNG in NSCLC specimens.

In conclusion, *ROS1* rearrangement was identified in 1.9% of surgically resected lung ADC, and it was more frequently found in younger women. The patients harboring *ROS1*-rearrangement showed shorter DFS than those with *ROS1* wild-type and *EGFR/KRAS/ALK/ROS1*-negative. *ROS1*-rearranged lung ADC exhibited distinct clinicopathological and morphological features, including high prevalence of cribriform and/or micropapillary pattern with aerogenous spread status and decreased membranous E-cadherin expression. Decreased membranous E-cadherin expression and aerogenous spread status may be associated with reduced DFS. Cutoff value of H-score 100 best predicts *ROS1* rearrangement. The criteria identified in this study

may allow ROS1 IHC to be used as a screening method to predict *ROS1* rearrangement. *ROS1* gene CNG is an independent factor of poor prognosis.

Reference

1. Jemal A, Bray F, Center MM, Ferlay J, Ward E, Forman D. Global cancer statistics. CA: a cancer journal for clinicians. 2011;61(2):69-90.

2. Scagliotti GV, Parikh P, von Pawel J, Biesma B, Vansteenkiste J, Manegold C, et al. Phase III study comparing cisplatin plus gemcitabine with cisplatin plus pemetrexed in chemotherapy-naive patients with advanced-stage non-small-cell lung cancer. Journal of clinical oncology : official journal of the American Society of Clinical Oncology. 2008;26(21):3543-51.

3. Sandler A, Gray R, Perry MC, Brahmer J, Schiller JH, Dowlati A, et al. Paclitaxel-carboplatin alone or with bevacizumab for non-small-cell lung cancer. The New England journal of medicine. 2006;355(24):2542-50.

4. Hoelder S, Clarke PA, Workman P. Discovery of small molecule cancer drugs: successes, challenges and opportunities. Molecular oncology. 2012;6(2):155-76.

5. Minuti G, D'Incecco A, Cappuzzo F. Targeted therapy for NSCLC with driver mutations. Expert opinion on biological therapy. 2013;13(10):1401-12.

6. Cardarella S, Johnson BE. The impact of genomic changes on treatment of lung cancer. American journal of respiratory and critical care medicine. 2013;188(7):770-5.

7. Birchmeier C, Birnbaum D, Waitches G, Fasano O, Wigler M. Characterization of an activated human ros gene. Molecular and cellular biology. 1986;6(9):3109-16.

8. Chin LP, Soo RA, Soong R, Ou SH. Targeting ROS1 with anaplastic lymphoma kinase inhibitors: a promising therapeutic strategy for a newly defined molecular subset of non-small-cell lung cancer. Journal of thoracic oncology : official

publication of the International Association for the Study of Lung Cancer. 2012;7(11):1625-30.

9. Davies KD, Doebele RC. Molecular pathways: ROS1 fusion proteins in cancer. Clinical cancer research : an official journal of the American Association for Cancer Research. 2013;19(15):4040-5.

10. Rikova K, Guo A, Zeng Q, Possemato A, Yu J, Haack H, et al. Global survey of phosphotyrosine signaling identifies oncogenic kinases in lung cancer. Cell. 2007;131(6):1190-203.

11. Birchmeier C, Sharma S, Wigler M. Expression and rearrangement of the ROS1 gene in human glioblastoma cells. Proceedings of the National Academy of Sciences of the United States of America. 1987;84(24):9270-4.

12. Peraldo Neia C, Cavalloni G, Balsamo A, Venesio T, Napoli F, Sassi F, et al. Screening for the FIG-ROS1 fusion in biliary tract carcinomas by nested PCR. Genes, chromosomes & cancer. 2014;53(12):1033-40.

13. Gu TL, Deng X, Huang F, Tucker M, Crosby K, Rimkunas V, et al. Survey of tyrosine kinase signaling reveals ROS kinase fusions in human cholangiocarcinoma. PloS one. 2011;6(1):e15640.

14. Birch AH, Arcand SL, Oros KK, Rahimi K, Watters AK, Provencher D, et al. Chromosome 3 anomalies investigated by genome wide SNP analysis of benign, low malignant potential and low grade ovarian serous tumours. PloS one. 2011;6(12):e28250.

15. Lee J, Lee SE, Kang SY, Do IG, Lee S, Ha SY, et al. Identification of ROS1 rearrangement in gastric adenocarcinoma. Cancer. 2013;119(9):1627-35.

16. Aisner DL, Nguyen TT, Paskulin DD, Le AT, Haney J, Schulte N, et al. ROS1 and ALK fusions in colorectal cancer, with evidence of intratumoral heterogeneity for

molecular drivers. Molecular cancer research : MCR. 2014;12(1):111-8.

17. Warth A, Muley T, Dienemann H, Goeppert B, Stenzinger A, Schnabel PA, et al. ROS1 expression and translocations in non-small-cell lung cancer: clinicopathological analysis of 1478 cases. Histopathology. 2014;65(2):187-94.

18. Go H, Kim DW, Kim D, Keam B, Kim TM, Lee SH, et al. Clinicopathologic analysis of ROS1-rearranged non-small-cell lung cancer and proposal of a diagnostic algorithm. Journal of thoracic oncology : official publication of the International Association for the Study of Lung Cancer. 2013;8(11):1445-50.

19. Govindan R, Ding L, Griffith M, Subramanian J, Dees ND, Kanchi KL, et al. Genomic landscape of non-small cell lung cancer in smokers and never-smokers. Cell. 2012;150(6):1121-34.

20. Takeuchi K, Soda M, Togashi Y, Suzuki R, Sakata S, Hatano S, et al. RET, ROS1 and ALK fusions in lung cancer. Nature medicine. 2012;18(3):378-81.

21. Seo JS, Ju YS, Lee WC, Shin JY, Lee JK, Bleazard T, et al. The transcriptional landscape and mutational profile of lung adenocarcinoma. Genome research. 2012;22(11):2109-19.

22. Shaw AT, Hsu PP, Awad MM, Engelman JA. Tyrosine kinase gene rearrangements in epithelial malignancies. Nature reviews Cancer. 2013;13(11):772-87.

23. Robinson DR, Wu YM, Lin SF. The protein tyrosine kinase family of the human genome. Oncogene. 2000;19(49):5548-57.

24. Ou SH, Bartlett CH, Mino-Kenudson M, Cui J, Iafrate AJ. Crizotinib for the treatment of ALK-rearranged non-small cell lung cancer: a success story to usher in the second decade of molecular targeted therapy in oncology. The oncologist. 2012;17(11):1351-75.

25. Bergethon K, Shaw AT, Ou SH, Katayama R, Lovly CM, McDonald NT, et al. ROS1 rearrangements define a unique molecular class of lung cancers. Journal of clinical oncology : official journal of the American Society of Clinical Oncology. 2012;30(8):863-70.

26. Kim H, Xu X, Yoo SB, Sun PL, Jin Y, Paik JH, et al. Discordance between anaplastic lymphoma kinase status in primary non-small-cell lung cancers and their corresponding metastases. Histopathology. 2013;62(2):305-14.

27. Salido M, Pijuan L, Martinez-Aviles L, Galvan AB, Canadas I, Rovira A, et al. Increased ALK gene copy number and amplification are frequent in non-small cell lung cancer. Journal of thoracic oncology : official publication of the International Association for the Study of Lung Cancer. 2011;6(1):21-7.

28. Seol-Bong Yoo HK, Xianhua Xu, Ping-Li Sun, Yan Jin. Jin Ho Paik, Sanghoon Jheon, Choon-Taek Lee, Jin-Haeng Chung. Clinicopathologic implications of ALK gene copy number gain in non-small cell lung cancer. J Lung Cancer. 2011;10(2):87-93.

29. Dacic S, Nikiforova MN. Present and future molecular testing of lung carcinoma. Advances in anatomic pathology. 2014;21(2):94-9.

30. Yoshida A, Kohno T, Tsuta K, Wakai S, Arai Y, Shimada Y, et al. ROS1-rearranged lung cancer: a clinicopathologic and molecular study of 15 surgical cases. The American journal of surgical pathology. 2013;37(4):554-62.

31. Jin Y, Sun PL, Kim H, Park E, Shim HS, Jheon S, et al. ROS1 gene rearrangement and copy number gain in non-small cell lung cancer. Virchows Archiv : an international journal of pathology. 2015;466(1):45-52.

32. Kim H, Jang SJ, Chung DH, Yoo SB, Sun P, Jin Y, et al. A comprehensive comparative analysis of the histomorphological features of ALK-rearranged lung

adenocarcinoma based on driver oncogene mutations: frequent expression of epithelial-mesenchymal transition markers than other genotype. PloS one. 2013;8(10):e76999.

33. Lira ME, Choi YL, Lim SM, Deng S, Huang D, Ozeck M, et al. A single-tube multiplexed assay for detecting ALK, ROS1, and RET fusions in lung cancer. The Journal of molecular diagnostics : JMD. 2014;16(2):229-43.

34. Yoshida A, Tsuta K, Wakai S, Arai Y, Asamura H, Shibata T, et al. Immunohistochemical detection of ROS1 is useful for identifying ROS1 rearrangements in lung cancers. Modern pathology : an official journal of the United States and Canadian Academy of Pathology, Inc. 2014;27(5):711-20.

35. Cha YJ, Lee JS, Kim HR, Lim SM, Cho BC, Lee CY, et al. Screening of ROS1 rearrangements in lung adenocarcinoma by immunohistochemistry and comparison with ALK rearrangements. PloS one. 2014;9(7):e103333.

36. Edge SB, Byrd DR, Compton CC, Fritz AG, Greene FL, Trotti A. AJCC cancer staging manual: Springer New York; 2010.

37. Travis WD, Brambilla, E., Burke, A.P., Marx, A., Nicholson, A. G. WHO Classification of Tumours of the Lung, Pleura, Thymus and Heart. 4th ed. Lyon: IARC Press2015.

38. Rogers TM, Russell PA, Wright G, Wainer Z, Pang JM, Henricksen LA, et al. Comparison of Methods in the Detection of ALK and ROS1 Rearrangements in Lung Cancer. Journal of thoracic oncology : official publication of the International Association for the Study of Lung Cancer. 2015;10(4):611-8.

39. Seo AN, Yang JM, Kim H, Jheon S, Kim K, Lee CT, et al. Clinicopathologic and prognostic significance of c-MYC copy number gain in lung adenocarcinomas. British journal of cancer. 2014;110(11):2688-99.

40. Cappuzzo F, Hirsch FR, Rossi E, Bartolini S, Ceresoli GL, Bemis L, et al. Epidermal growth factor receptor gene and protein and gefitinib sensitivity in non-small-cell lung cancer. Journal of the National Cancer Institute. 2005;97(9):643-55.

41. Travis WD, Brambilla E, Noguchi M, Nicholson AG, Geisinger KR, Yatabe Y, et al. International association for the study of lung cancer/american thoracic society/european respiratory society international multidisciplinary classification of lung adenocarcinoma. Journal of thoracic oncology : official publication of the International Association for the Study of Lung Cancer. 2011;6(2):244-85.

42. Lee HJ, Xu X, Kim H, Jin Y, Sun P, Kim JE, et al. Comparison of Direct Sequencing, PNA Clamping-Real Time Polymerase Chain Reaction, and Pyrosequencing Methods for the Detection of EGFR Mutations in Non-small Cell Lung Carcinoma and the Correlation with Clinical Responses to EGFR Tyrosine Kinase Inhibitor Treatment. Korean journal of pathology. 2013;47(1):52-60.

43. Chung JH, Choe G, Jheon S, Sung SW, Kim TJ, Lee KW, et al. Epidermal growth factor receptor mutation and pathologic-radiologic correlation between multiple lung nodules with ground-glass opacity differentiates multicentric origin from intrapulmonary spread. Journal of thoracic oncology : official publication of the International Association for the Study of Lung Cancer. 2009;4(12):1490-5.

44. Paik JH, Choi CM, Kim H, Jang SJ, Choe G, Kim DK, et al. Clinicopathologic implication of ALK rearrangement in surgically resected lung cancer: a proposal of diagnostic algorithm for ALK-rearranged adenocarcinoma. Lung cancer (Amsterdam, Netherlands). 2012;76(3):403-9.

45. Sun PL, Seol H, Lee HJ, Yoo SB, Kim H, Xu X, et al. High incidence of EGFR mutations in Korean men smokers with no intratumoral heterogeneity of lung adenocarcinomas: correlation with histologic subtypes, EGFR/TTF-1 expressions, and

clinical features. Journal of thoracic oncology : official publication of the International Association for the Study of Lung Cancer. 2012;7(2):323-30.

46. Motoi N, Szoke J, Riely GJ, Seshan VE, Kris MG, Rusch VW, et al. Lung adenocarcinoma: modification of the 2004 WHO mixed subtype to include the major histologic subtype suggests correlations between papillary and micropapillary adenocarcinoma subtypes, EGFR mutations and gene expression analysis. The American journal of surgical pathology. 2008;32(6):810-27.

47. Kadota K, Yeh YC, D'Angelo SP, Moreira AL, Kuk D, Sima CS, et al. Associations between mutations and histologic patterns of mucin in lung adenocarcinoma: invasive mucinous pattern and extracellular mucin are associated with KRAS mutation. The American journal of surgical pathology. 2014;38(8):1118-27.

48. Rekhtman N, Ang DC, Riely GJ, Ladanyi M, Moreira AL. KRAS mutations are associated with solid growth pattern and tumor-infiltrating leukocytes in lung adenocarcinoma. Modern pathology : an official journal of the United States and Canadian Academy of Pathology, Inc. 2013;26(10):1307-19.

49. Sholl LM, Sun H, Butaney M, Zhang C, Lee C, Janne PA, et al. ROS1 immunohistochemistry for detection of ROS1-rearranged lung adenocarcinomas. The American journal of surgical pathology. 2013;37(9):1441-9.

50. Hung JJ, Jeng WJ, Chou TY, Hsu WH, Wu KJ, Huang BS, et al. Prognostic value of the new International Association for the Study of Lung Cancer/American Thoracic Society/European Respiratory Society lung adenocarcinoma classification on death and recurrence in completely resected stage I lung adenocarcinoma. Annals of surgery. 2013;258(6):1079-86.

51. Yoshizawa A, Motoi N, Riely GJ, Sima CS, Gerald WL, Kris MG, et al.

Impact of proposed IASLC/ATS/ERS classification of lung adenocarcinoma: prognostic subgroups and implications for further revision of staging based on analysis of 514 stage I cases. Modern pathology : an official journal of the United States and Canadian Academy of Pathology, Inc. 2011;24(5):653-64.

52. Kodama K, Ishii G, Miyamoto S, Goya M, Zhang SC, Sangai T, et al. Laminin 5 expression protects against anoikis at aerogenous spread and lepidic growth of human lung adenocarcinoma. International journal of cancer Journal international du cancer. 2005;116(6):876-84.

53. Yang YL, Chen MW, Xian L. Prognostic and clinicopathological significance of downregulated E-cadherin expression in patients with non-small cell lung cancer (NSCLC): a meta-analysis. PloS one. 2014;9(6):e99763.

54. Pan Y, Zhang Y, Li Y, Hu H, Wang L, Li H, et al. ALK, ROS1 and RET fusions in 1139 lung adenocarcinomas: a comprehensive study of common and fusion pattern-specific clinicopathologic, histologic and cytologic features. Lung cancer (Amsterdam, Netherlands). 2014;84(2):121-6.

55. Chen YF, Hsieh MS, Wu SG, Chang YL, Shih JY, Liu YN, et al. Clinical and the Prognostic Characteristics of Lung Adenocarcinoma Patients with ROS1 Fusion in Comparison with Other Driver Mutations in East Asian Populations. Journal of thoracic oncology : official publication of the International Association for the Study of Lung Cancer. 2014;9(8):1171-9.

56. Lee SE, Lee B, Hong M, Song JY, Jung K, Lira ME, et al. Comprehensive analysis of RET and ROS1 rearrangement in lung adenocarcinoma. Modern pathology : an official journal of the United States and Canadian Academy of Pathology, Inc. 2015;28(4):468-79.

57. Mescam-Mancini L, Lantuejoul S, Moro-Sibilot D, Rouquette I, Souquet PJ,

Audigier-Valette C, et al. On the relevance of a testing algorithm for the detection of ROS1-rearranged lung adenocarcinomas. Lung cancer (Amsterdam, Netherlands). 2014;83(2):168-73.

58. Camidge DR, Skokan M, Kiatsimkul P, Helfrich B, Lu X, Baron AE, et al. Native and rearranged ALK copy number and rearranged cell count in non-small cell lung cancer: implications for ALK inhibitor therapy. Cancer. 2013;119(22):3968-75.

Table 1. Clinicopathological characteristics of the patients

Characteristics		Patients, No. (%)
Sex	Male	501 (66.4%)
	Female	253 (33.6%)
Age (years)	Median (Range)	66 (23-85)
Smoking history	Never	303 (40.2%)
	Ex-smoker	114 (15.1%)
	Current smoker	337 (44.7%)
Tumor size (cm)	Mean (Range)	3.5 (0.8-16)
Histology subtype	ADC	469 (62.2%)
	SqCC	254 (33.7%)
	Others	31 (4.1%)
Pleural invasion	Absent	451 (59.8%)
	Present	303 (40.2%)
Vascular invasion	Absent	566 (75.1%)
	Present	188 (24.9%)
Lymphatic invasion	Absent	388 (51.5%)
	Present	366 (48.5%)
p-Stage	I	361 (47.9%)
	II	188 (25.0%)
	III	172 (22.8%)
	IV	33 4.4%)
Total		754

Abbreviations: ADC, adenocarcinoma; SqCC, squamous cell carcinoma; p-Stage, pathological stage

Table 2. Clinicopathological features of patients with ROS1-rearranged NSCLC

No.	Sex	Age	Size (mm)	Smoking	Histology	Subtype	p-Stage	FISH + cells (%) (BA/IGS)	Aerogenous spread	*EGFR/KRAS/ALK* mutation
1	M	52	28	ex-smoker	ADC	acinar, micropapillary, cribriform pattern	Ib	32 (24/8)	+	-/-/-
2	F	58	35	non-smoker	ADC	acinar, micropapillary, cribriform pattern	Ib	58 (38/20)	+	-/-/-
3	M	56	43	ex-smoker	ADC	micropapillary, papillary, cribriform patter	IIIa	58 (46/12)	+	-/-/-
4	F	58	48	non-smoker	ADC	micropapillary, papillary	IV	17 (15/2)	+	-/-/-
5	F	50	26	non-smoker	ADC	solid with signet ring cell and mucinous cribriform pattern	IIIa	56 (34/22)	+	-/-/-
6	F	80	25	non-smoker	ADC	solid, micropapillary	Ib	68 (40/28)	+	-/-/-
7	M	55	41	current-smoker	ADC	acinar, micropapillary	IV	62 (46/16)	+	-/+/-
8	F	51	41	non-smoker	ADC	solid, acinar	IIIa	56 (27/29)	+	-/-/-
9	F	71	28	non-smoker	ADC	lepidic, acinar	Ia	58 (46/11)	+	-/-/-
10	F	45	25	non-smoker	PC	ADC + sarcomatous	IIa	52 (37/15)	+	-/-/-

Abbreviations: M, male; F, female; ADC, adenocarcinoma; PC, pleomorphic carcinoma; BA, break-apart signal; IGS, isolated green(3’ end) signal; EGFR, epidermal growth factor receptor; KRAS, kirsten rat sarcoma viral oncogene homolog; ALK, anaplastic lymphoma kinase.

Table 3. Association between clinicopathological features and ROS1 gene rearrangement

	Total (n = 754)	*ROS1* FISH		*P* value
		Positive (%)	Negative (%)	
Sex				
Male	501	3(0.6)	498(99.4)	0.014
Female	253	7(2.8)	246(97.2)	
Age				
≤65	362	8(2.2)	354(97.8)	0.042
>65	392	2(0.5)	390(99.5)	
Smoking				
No	303	7(2.3)	296(97.7)	0.053
Yes	451	3(0.7)	448(99.3)	
Tumor size (mm)				
≤30	390	5(1.3)	385(98.7)	0.913
>30	364	5(1.4)	359(98.6)	
Histology				
ADC	469	9(1.9)	460(98.1)	0.063
SqCC	254	0(0.0)	254(100.0)	
Others	31	1(3.2)	30(96.8)	
Pleural invasion				
Absent	451	3(0.7)	448(99.3)	0.053
Present	303	7(2.3)	296(97.7)	
p-Stage				
I	361	4(1.1)	356(98.9)	0.074
II	188	1(0.5)	188(99.5)	
III	172	3(1.7)	169(98.3)	
IV	33	2(6.1)	31(93.9)	

Table 4. Performance of ROS1 IHC analysis to predict gene rearrangement

Criteria	*ROS1*-rearranged cases (n = 10)	*ROS1* wild-type cases (n = 744)	Sensitivity	Specificity
H-score				
≥50	9	107	90.0%	85.6%
≥80	9	83	90.0%	88.8%
≥100	9	48	90.0%	93.5%
≥150	8	22	80.0%	97.0%
≥200	7	2	70.0%	99.7%
Extent				
≥10%	9	171	90.0%	77.0%
≥20%	9	121	90.0%	83.7%
≥50%	9	95	90.0%	87.2%
≥75%	9	61	90.0%	91.8%
Intensity				
≥1+	9	199	90.0%	73.3%
≥2+	8	78	80.0%	89.5%
≥3+	6	3	60.0%	99.6%

Table 5. Multivariate Cox proportional hazards analysis

	Disease-free survival			Overall survival		
Variable	**HR**	**95% CI**	***P* value**	**HR**	**95% CI**	***P* value**
Pleural invasion						
Absent vs. Present	1.49	1.08–2.04	0.014	1.37	0.91–2.08	0.134
p-Stage						
I + II vs. III + IV	3.14	2.28–4.33	<0.001	5.28	3.41–8.18	<0.001
***ROS1* gene CNG**						
Positive vs. Negative	2.16	1.22–3.81	0.008	2.53	1.31–4.89	0.006

Abbreviations: HR, hazard ratio; CI, confidence interval

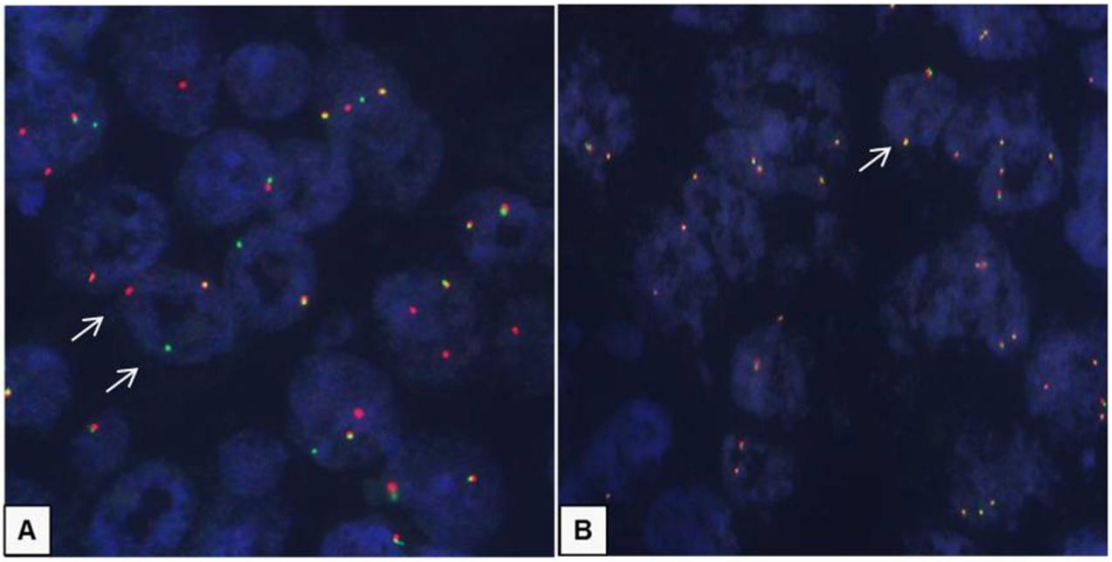

Figure 1. Representative images of *ROS1* FISH. *ROS1* rearranged tumor either showed a split one or more signal widths apart between the orange and green signals or a single green signal (A) and *ROS1* wild-type tumor showed fused orange and green signals (B).

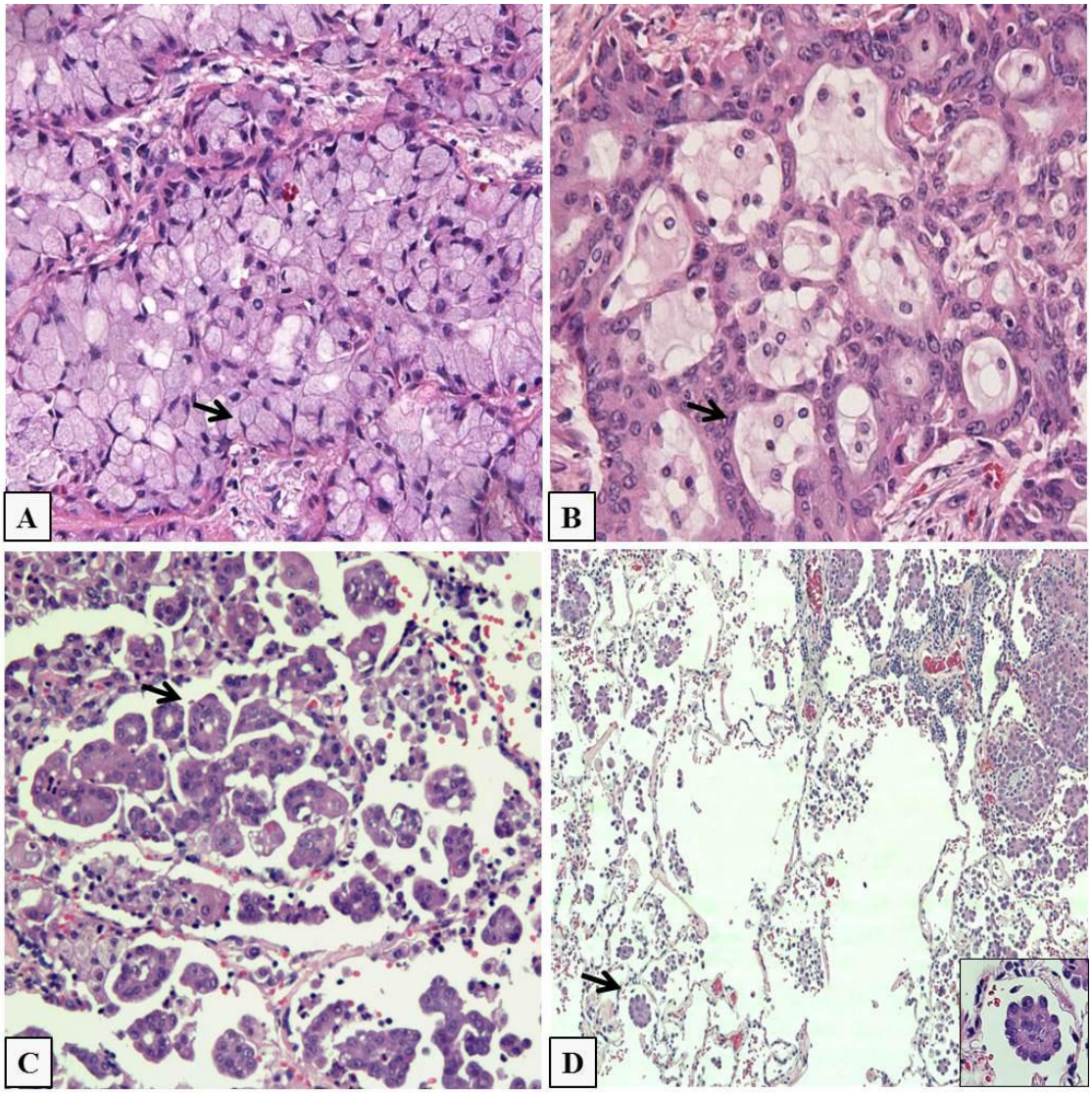

Figure 2. Histological features of *ROS1*-rearranged tumors. Representative images of solid growth patterns containing signet ring cell components (**A**), a cribriform pattern (**B**), a micropapillary component (**C**), and aerogenous spread (**D**).

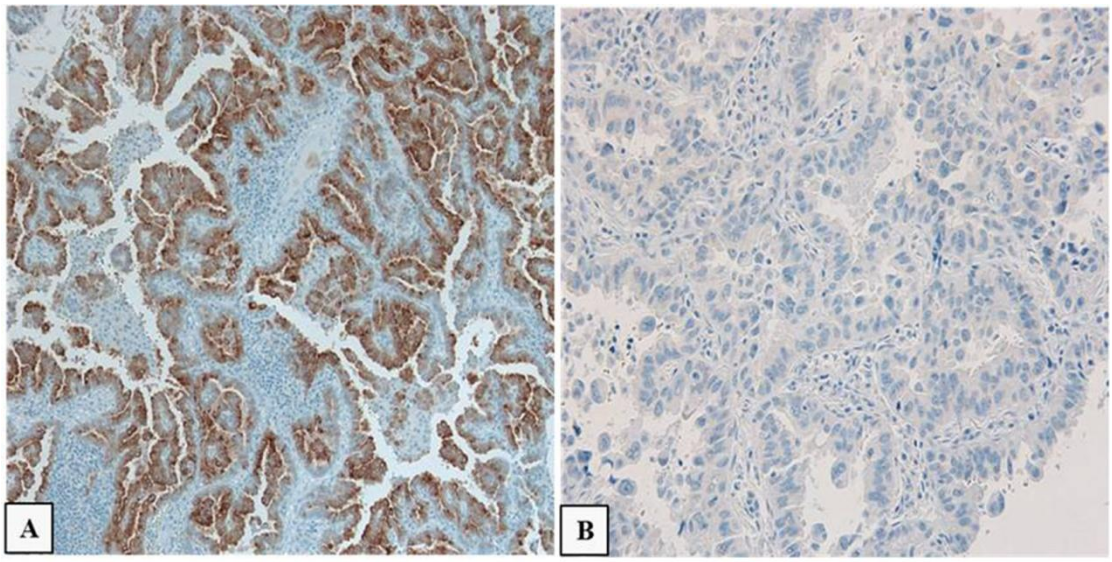

Figure 3. Representative images of ROS1 IHC in *ROS1*-rearranged and wild-type tumors. Immunohistochemistry of ROS1: a case with *ROS1*-rearranged tumor showed strong and diffuse staining (A) and a case with *ROS1* wild-type tumor showed the absence of ROS1 reactivity (B)

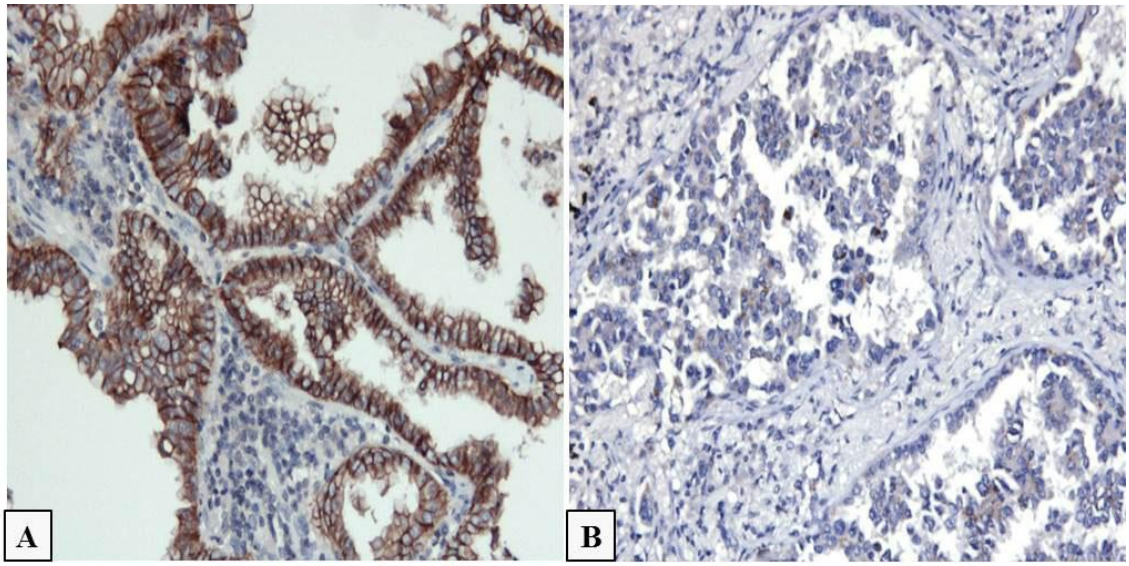

Figure 4. Representative images of E-cadherin protein expression in *ROS1*-rearranged and wild-type tumors. Immunohistochemistry of E-cadherin, normal circumferential membrane staining pattern in *ROS1* wild-type tumor (**A**) and decreased membranous staining pattern in *ROS1*-rearranged tumors with a micropapillary component (**B**).

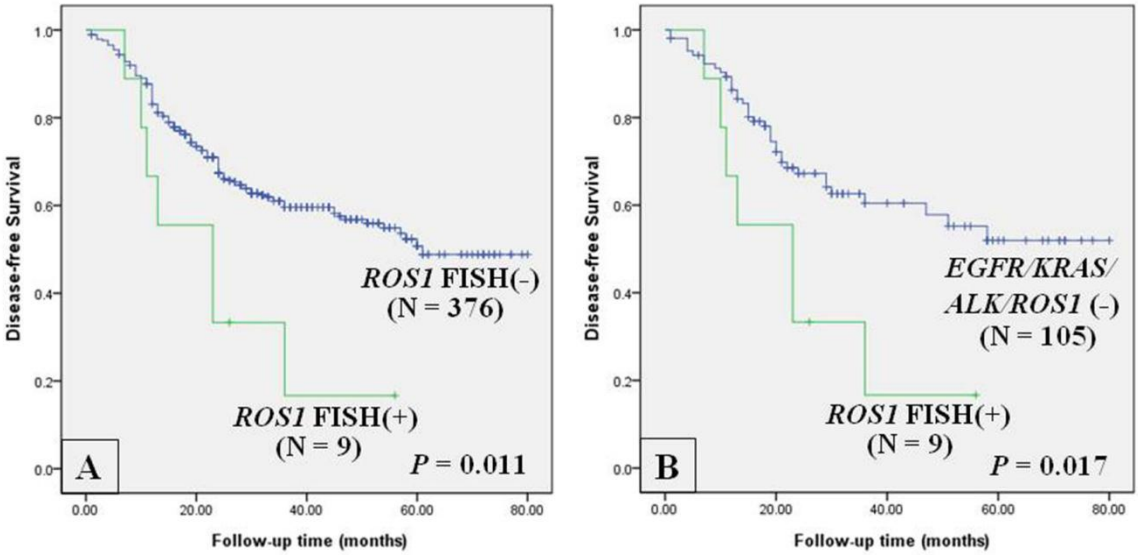

Figure 5. Kaplan-Meier univariate analysis of disease-free survival curves based on *ROS1* rearrangement in adenocarcinoma patients. Patients with *ROS1* rearrangement tumor had significantly shorter disease-free survival than did patients with *ROS1* wild-type tumor (**A**) and *EGFR/KRAS/ALK/ROS1*-negative adenocarcinoma (**B**).

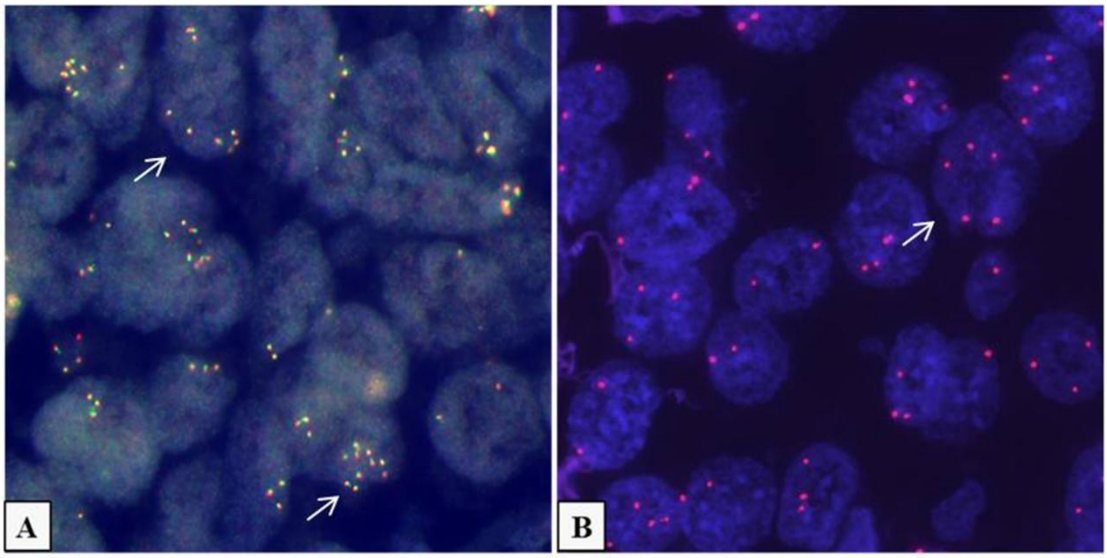

Figure 6. Representative images of *ROS1* gene copy number gain and CEP6 status. A case with *ROS1* gene copy number gain showed increased fusion signals (A) and a case with CEP6 copy number gain showed mean CEP6 ≥ 3 copies per nucleus (B).

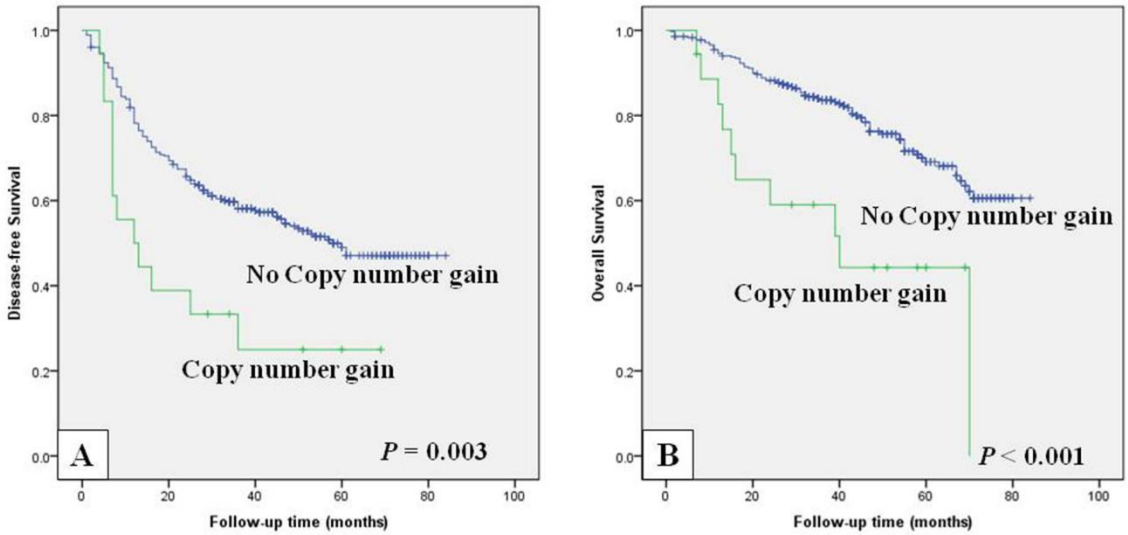

Figure 7. Kaplan-Meier univariate analysis of disease-free survival and overall survival curves in NSCLC patients. *ROS1* gene copy number gain was significantly associated with a higher risk of recurrence (A) and shorter overall survival (B).

국문초록

서론: 최근 *ROS1* 유전자 변이가 특정 폐암 환자군에서 강력한 발암 인자로 밝혀졌고, ALK와 같은 TKI치료제인 crizotinib을 이용한 임상 시험에서 현저한 종양 억제 효과를 보임으로서 *ROS1* 유전자 전위가 각광을 받고 있다. 본 연구에서는 비소세포폐암에서 *ROS1* 유전자 전위의 발생빈도, 임상병리학적 및 기타 driver oncogene과 구분되는 형태학적 소견을 분석하고 *ROS1* 유전자 copy number gain (CNG)의 임상병리학적 의의를 규명하고자 했다. 또한 *ROS1* 유전자 전위 양성 비소세포폐암을 신속 정확하게 진단하는 조직면역화학적 방법을 찾고자 한다.

연구대상 및 방법: 754명의 비소세포폐암에서 형광제자리부합법 (fluorescent in situ hybridization)을 통해 *ROS1* 유전자 변이를 관찰하고 면역조직화학기법 (immunohistochemistry)으로 ROS1과 E-cadherin 단백발현을 관찰하였다.

결과: 총 754명의 폐암증례 중 10례의 *ROS1* 유전자 전위가 관찰되었다 (1.3%, NSCLC; 1.9%, ADC). 조직학적으로, 상기 10례의 증례는 모두 adenocarcinomatous component를 포함하고 있다. *ROS1* 유전자 전위는 미세유두형 패턴 (micropapillary pattern)의 존재, 공기확산상태 (aerogenous spread status), 및 E-cadherin 소실과 상관관계를 보였다. Kaplan-Meier 생존분석결과 *ROS1* 유전자 전위는 통계학적 유의하게 높은 재발이 확인되었다. 9례의 증례에서 중간정도 혹은 강한 ROS1 면역반응성을 보였지만 이에 반해 *ROS1* wild-type 폐암에서는 대부분이 면역반응성을 보이지 않았다. 면역염색을 통해 *ROS1* 유전자 전위를 정확하게 예측할 수 있는 알맞은 기준으로는 H-score ≥100, 이때 민감도와 특이도가 각각 90%와 93.5%로 확인되었다. 총 4.8%증례에서 *ROS1* 유전자 CNG을 보였고 이런 환자는 통계학적 유의하게 높은 재발과 짧은 생존을 보였고, 무병생존율과 전체생존율에 대한 다변량분석

(multivariate analysis) 결과, *ROS1* 유전자 CNG은 독립적인 나쁜 예후인자로 작용함을 확인할 수 있었다.

결론: *ROS1* 유전자 전위 폐선암은 특유의 임상병리학적특성 및 조직학적 소견을 보였다. E-cadherin 소실과 공기확산은 환자의 짧은 무병생존율을 초래하게 되는 원인 중 하나라고 추측할 수 있다. 또한, *ROS1* 유전자 CNG은 수술적으로 절제된 비소세포폐암에서 독립적인 나쁜 예후인자로 작용한다.

주요어: 폐암, *ROS1* 유전자 변이, 조직형태학, 면역조직화학기법

학번: 2012-31337